

EFFECT OF NOZZLE DESIGN ON ALUMINUM POWDER PRODUCED BY LABORATORY SCALE ATOMIZER

Agada S. O. ^{a*}, Abdulrahman, A. S. ^b, Abolarin, M. S. ^a, Egbe, E. A.P. ^a, Abutu J. ^a

^aDepartment of Mechanical Engineering, School of Infrastructure, Process and Engineering Technology,
Federal University of Technology, Minna- Nigeria

^bDepartment of Material and Metallurgical Engineering, School of Infrastructure, Process and Engineering
Technology, Federal University of Technology, Minna- Nigeria

*Corresponding author email: joe4abutu@gmail.com. Phone: +2347035241729

ABSTRACT

Poor nozzle design affects the quantity of the aluminium powder produced from a laboratory scale atomizer. This is as a result of the non-optimization of the atomizing fluid required to cause effective disintegration of the melt stream into particulate powder. In order to maintain thin stable melt film droplet for enhancing the particle size distribution, this study investigates the influence of variation in the angle of attack of pressurised air medium on a designed laboratory-scale air atomizer for producing aluminium powders. Particle mean diameter ranging from 3 - 200 μ m was obtained for 40° angle of attack, 14 mm nozzle diameter, and 12bar operating pressure, while particle mean diameter ranging from 75-250 μ m was obtained for 45° angle of attack at the same operating conditions. The result shows that 40° angle of attack produced optimum yield Aluminium powder. Also, the disintegration mechanism, solidification behaviour, and powder properties were in agreement with previous research works on air atomization process. The implication of the findings from this study confirms the attainment of the appropriate angle of attack (40°) of the atomizing medium in producing aluminium powders having narrow size distribution at higher production efficiency and low costs.

Keywords: Atomization; Angle of attack; Aluminium powder; Solidification behaviour; Film disintegration.

1.0 INTRODUCTION

Increasing world-wide adoption of powder metallurgy (PM) products is hinged on its merits such as high productivity, homogeneous microstructure associated with enhanced mechanical properties, energy saving, and attainment of near net-shape parts which are quite impossible with the conventional ingot metallurgy production routes [1]. Nevertheless, the practice of PM in Nigeria is at its lowest ebb as a result of shortage of human resources and non-development of the technical- know how in the field of PM over the years. Consequently, this has constituted a big burden to the Nigerian PM Industry development and international competitiveness. However, PM industries are currently faced with the challenge of enhancing efficient productivity and economy of conventional atomization processes for producing metal

powders. In order to combat this challenge, different variants of atomization techniques have been developed: high pressure inert gas atomization (HPIGA), ultrasonic gas atomization (USGA), centrifugal spinning atomization (CSA), high pressure gas centrifugal rotation disc (HPGCRD), centrifugal hydraulic atomization (CHA), and two-stage quenching atomization (TSQA) for the production of powders with varying particle morphologies and structures [2][3][4][5] and [6]. However, these variants of atomization process are considered to be expensive due to the use of expensive equipment and inert gases as well as the production of powders with wide particle size distribution. Hence, the adoption of low cost air atomization process with high mass flow rate in this study for producing aluminium powders for various applications.

Also, air atomization process is faced with the challenge of producing only a small fraction of the raw metal powder that can only be used as a product thereby necessitating that larger and smaller particle size distribution must be separated. The production of powders with wide particle size distribution translates to lower productivity for the PM businesses. Anderson *et al.*, [7] attributed the production of powders having wide particle size distribution to the instability of the melt film at the nozzle tip as a result of non-optimization of the physical contact between the air and the liquid melt. Possible solution towards optimizing the physical contact between the air and the liquid melt is by varying the angle of attack of the atomizing medium on the melt film. Therefore, in order to address all these challenges, this study is aimed at developing laboratory scale atomization equipment for producing aluminium powders with a view to educating young Nigerian undergraduates. This is anticipated to motivate students in developing their skills and knowledge for future employment in the PM industry. Also, the variation of the angle of attack of the atomizing medium in the nozzle design on the melt film was also investigated in order to produce a stable melt film. It is expected that the determination of the appropriate angle of attack of the air atomizing medium will maintain a thin film of more stable melt droplet resulting in narrow particle size distribution at a lower production costs and improved productivity. However, at an inappropriate angle of attack of the atomizing medium, air atomization process will produce undesirable larger mean particle sizes.

2.0 MATERIALS AND DESIGN METHODOLOGY

2.1 Design of the Air Atomization Equipment

a. The Furnace Tundish

The furnace tundish used was made of cast iron with truncated pyramid geometry of

2mm thickness to accommodate 10kg of aluminium melt as shown in Fig. 1a. This material was selected as a result of its low cost, ability to withstand a maximum operating temperature of 800°C, high oxidation resistance at 1000 °C, and high mechanical strength at 900 °C. An actuator was also introduced to control the opening at the bottom of the tundish so that the melt flows into the nozzle duct at a regulated quantity (Fig. 1b). The slag covers the melt so that it acts as a de-oxidant to prevent oxygen from coming in contact with the melt.

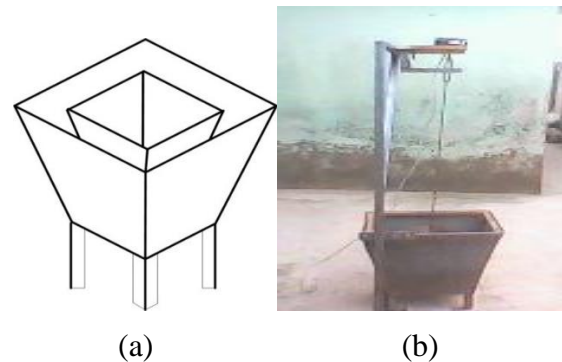


Fig. 1: The furnace design

b. The Nozzle

The nozzle is made up of an annular shape (Fig. 2) and steel pipe with cast aluminium metal material. Aluminium material was selected as a result of its workability, availability, cost and low operating temperature. Also, the passage of heat at 800°C will prevent the breakdown of nozzle since it is always in contact with the natural (convection) moving atomizing air external and Conductive medium air internally. Equ. 2 adopted by Lubanska [8] was employed to determine the mean particle diameter ($d_m = 169 \mu\text{m}$).

Also, Table 1 shows the design parameters used in determining the mean particle diameter. These parameters were utilized in the fabrication and development of the atomizer.

$$d_m = d_t K \left[\frac{v_m}{v_a} (1 + M/G) / W_s \right]^{1/2} \quad (1)$$

Fig. 2 shows how the variation in the angle of attack of the atomizing medium under constant operating conditions influences the atomization process. Fig. 2a depicts how the shearing force of the atomizing medium at 45° causes eddies and blocks the melt from falling under gravity thereby resulting in large particles of aluminum powders with voids whereas Fig. 2b reveals that when the angle of attack of the atomizing medium was reduced to 40° , smaller sized particles were produced.

Moreover, it could be seen that the stability of the liquid stream –that is, its length prior to breakup–increases with increase in diameter of the stream as the angle of attack of the atomizing medium was reduced to 40° . Therefore, by decreasing angle of attack of the atomizing medium to 40° , the flow transition from turbulent to laminar was noted to have improved jet stability. The fabricated close coupled nozzle is shown in Fig. 3.

Table 1: Design parameters used in determining the mean particle diameter.

d_m	Mass median particle diameter (μm)	169
d_t	Diameter of the atomizer nozzle or the liquid stream diameter (m),	0.014
ν_m	kinematic viscosities of the molten metal ($\text{m}^2 \text{s}^{-1}$)	4.8E-9
ν_a	kinematic viscosities of the atomizing medium ($\text{m}^2 \text{s}^{-1}$)	14.78E-6
M	Mass flow rates of the metal (kg s^{-1}).	8.64
G	Mass flow rates of the atomizing medium (g s^{-1}).	11
G'	Atomizing medium flow rate in L/s with $G = ((G'/1000) \rho_a)/60$	106.24
K	Experimentally determined constant (at 12 bar)	14.5
W_e	Weber's number $W_e = V^2 \rho d_t / \sigma$	10.5E5
V	velocity ($V = G/S\rho_a$) m/s	155.22
ρ	Density of the metal (kgm^{-3}),	2.700
ρ_a	Density of the atomizing medium (kgm^{-3})	1.225
σ	Surface tension of the liquid metal (kg s^{-2})	0.869
S	Surface of the crown of the atomizing medium (m^2).	6.2E-4

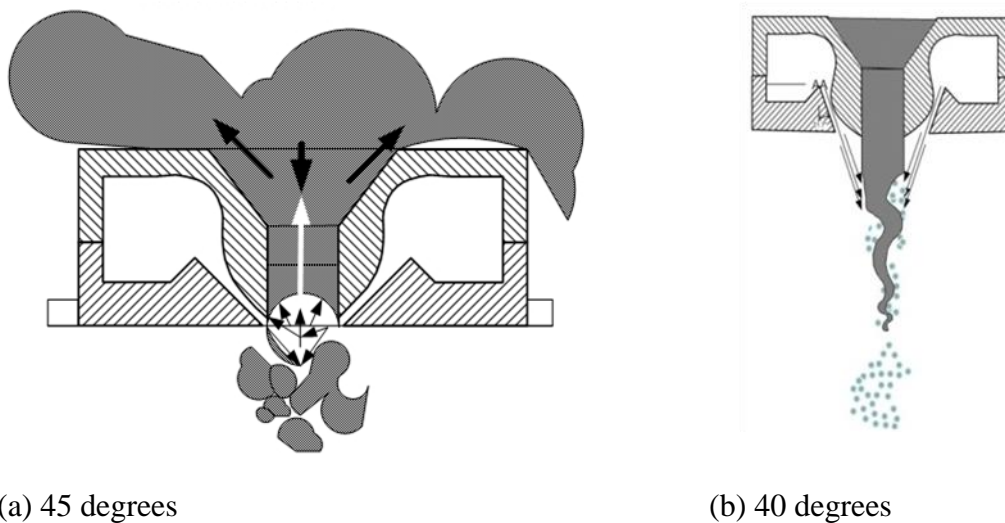


Fig. 2: Design of the nozzles with different incidence angles



Fig. 3: Fabricated Closed Coupled nozzle

c. The Atomizing Chamber

The atomizing chamber was developed from a sheet of cast steel of 2mm diameter using American Society of Mechanical Engineer (ASME) Boiler code (SA 516 Gr 75 UG-36). The atomizing chamber was formed using a sheet roller seamlessly welded to form a cylindrical atomizer unit as shown in Fig.4



Fig. 4: Fabricated atomizing chamber

d. The Powder Collector

The geometry of truncated cone was adopted for the powder collection chamber due to the ease of fabrication with the available tools. It was made of steel metal sheet of 2 mm thickness. The fabricated collector chamber is shown in Fig. 5.



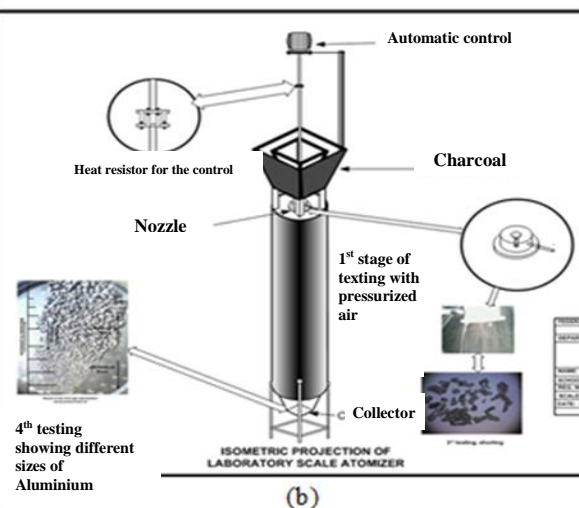
Fig. 5: Fabricated collector chamber

2.2 Fabrication of the Air Atomiser Equipment

The fabrication of the air atomiser for producing aluminium powders involved marking out, cutting, drilling, machining, filling, pattern/mould making, turning and welding of the component parts. Fig.6 (a and b), represent the assembly of the various components and isometric drawing of the air atomiser respectively.



(a)



(b)

Fig. 6: Assembly of the various components of the air atomizer and its Isometric view

2.3. Operation of the Air Atomiser Equipment

Similar to the atomiser designed by Plancheet *al.* [9], the atomization of the liquid metal could be attributed to the laminar flow effect of the air within the atomizing area reaching sonic or supersonic speed [10]. The equipment is composed of the melt nozzle and the

atomizing nozzle of which its design lead to the build-up of negative over pressure at the tip of the melt nozzle. The aluminium melted in the tundish which is separated from the atomization chamber by the atomizing nozzle so that the tundish is pressurised during the atomization process and also acts as a buffer tank. The molten aluminium stream flows out of the bottom of the tundish under the static height of the melt in the crucible and the negative overpressure at the melt nozzle tip. At the exit of the tundish, the liquid aluminium stream meets the cold and pressurised air. Consequently, the melt monofilament becomes thin due to the action of the shear forces exerted by the atomizing air, thereby commencing the process of atomization. As the atomization process progresses, the monofilament explodes into many monofilaments or droplets and solidify during their flight downstream in the atomizing chamber or collection tray. The need to maintain melt superheat in the duct is critically important as it is necessary that melt flow should exit the duct for the progression of the atomization process [11]. To achieve this, it was ensured that air pressure in the tundish was not held constant throughout the atomization process as the pressure was increased from the start of the flow to the desired atomization pressure. Therefore, the melt flow was initiated at a pressure below the desired atomization pressure with a view to avoiding solidification of the melt in the melt nozzle. Immediately the desired atomization pressure was attained, a good stability of this pressure was then obtained with less than 10%.

2.4 Disintegration Mechanism of the Aluminium Melt Droplets

In order to gain an understanding of how the melt droplets will disintegrate into powders and make amends for any observed difficulty that may arise during the actual operation of the atomizer with molten metal droplets, it was decided that soapy water be introduced under high pressure of 12 bar and 40° angle of attack.

As shown in Fig. 7, it was observed that as the soapy bubbles emerged from the nozzle duct, the impingement of the air on the droplets of soapy bubbles caused it to fragment to smaller sizes of bubbles by a shearing effect.



Fig. 7: Spray geometry using soapy water and air for simulating atomization

A careful observation of the fragmentation process of the bubbles as shown in Fig. 7 revealed that at higher air pressure, the bubbles disintegrated into smaller bubble particles to form a cone shaped geometry. The disintegration mechanism of the aluminium melt droplets is shown in Fig. 8.

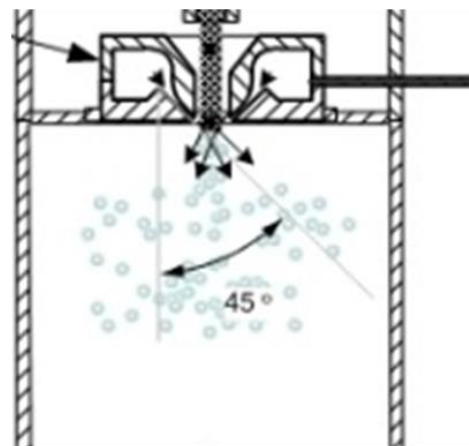


Fig. 8: Disintegration of aluminum melt droplets mechanism

Five stages of disintegration mechanism associated with air atomization are observed in Fig. 8. This includes:

- i. Wave formation through initiation of small disturbance at the surface of the liquid

- ii. Wave fragment and ligament formation through shearing forces on the disturbances of stage I
- iii. Breakdown of ligaments into droplets (primary atomization); regular particle shape favored by high surface tension and low cooling rate; irregular particle shape by low surface tension and high cooling rate
- iv. Further deformation and thinning of droplets and wave fragments into smaller particles (secondary atomization)
- v. Collision and coalescence of particles

2.5 Solidification Behaviour of the Aluminium Melt Droplets

Similar to the approach adopted by Fuqian *et al.*, [2] in order to estimate the solidification rate of the powder, the solidification process was categorised as follows;

Stage I: Determination of the heat transfer between pressurised air and molten droplets

Stage II: Determination of the heat transfer between liquid (usually water), and solidified droplets

According to Fuqian *et al.*, [2], the heat transfer (h) between the air and the molten droplets was determined using Equ. 3. Fuqian *et al.*, [2]

$$h = K_a / d_m [2.0 + 0.6 \left(\frac{V d_m \rho_a}{\eta_a} \right)^{\frac{1}{2}} \left(\frac{C_a \eta_a}{K_a} \right)^{\frac{1}{2}}] \quad (3)$$

Where, K_a is the thermal conductivity of air, d_m the diameter of a droplet, V the relative velocity between air and droplet, ρ_a the density of the air, C_a the thermal capacity of the air and η_a is the dynamic viscosity of air. The author also reported that if the relative velocity (V) was approximately equal to zero during atomization process, the heat transfer (h) is represented as shown in Equ.4 Fuqian *et al.*, [2].

$$h = 2 \frac{K_a}{d_m} \quad (4)$$

Considering the principle of thermal conduction, solidification time t_s could be calculated using Equ. 5 Fuqian *et al.*, [2].

$$t_s = \frac{\Delta H}{h \Delta T_c A} \quad (5)$$

Where, ΔH is the quantity of heat when droplet solidified, ΔT_c represent the difference of temperature between droplet and environment and A is the area of droplet. The quantity of heat (ΔH) is as shown in Equ. 6 Fuqian *et al.*, [2].

$$\Delta H = V_{droplet} (C_1 \Delta T_s + \Delta H_f) \quad (6)$$

Where $V_{droplet}$ is the volume of droplet, C_1 the specific heat of molten aluminium, ΔT_s represent the overheat temperature molten metal and ΔH_f is the latent heat. Hence, the cooling rate is determined from Equ. 6 Fuqian *et al.*, [2].

$$dT/dt = \Delta T / t_s \quad (7)$$

3.0 RESULTS AND DISCUSSION

3.1 Powder properties

Fig. 9 (a and b) reveals the effects of varying the incidence angle on the caking, particle mean size and shape of powders produced.



(a) Powder particles produced at 45°



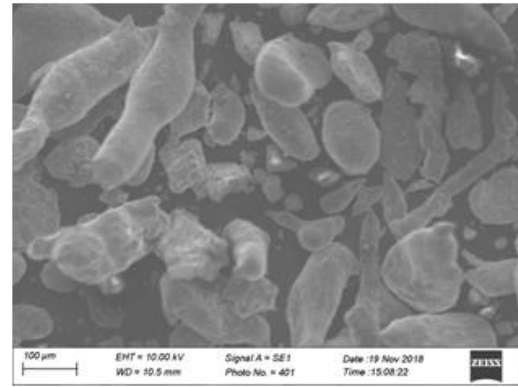
(b) Powder particles produced at 40°

Fig. 9: Effect of variation of angle of attack of the atomizing medium on the quantity of powder produced using fabricated nozzles

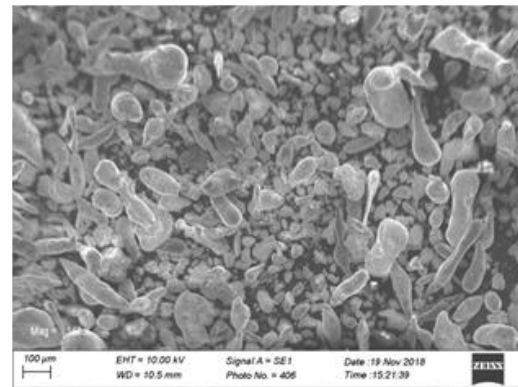
Fig. 9(a) reveals that at 45° lower yield and clumping or caking was experienced at the nozzle tip of a closed-coupled nozzle due to the geometrical intersection of the high velocity cooling air medium with the melt stream which became unstable, and freezes the melt stream faster leading to the perspiration pressure which causes melt flow back. Caking was observed from 45° incidence and above. Also, Fig. 9(b) shows a more stable bombardment of the melt stream by an incidence angle of 40° which did not allow for intersection of the high velocity atomizing medium, this provides a stable sinusoidal wave action on the melt stream instead leading to a more catastrophic break down of the ligaments as proposed by the Downbroski model [13]. Both powders obtained from the use of this atomizer as shown in Fig 9 (a and b) shows variations in quantity, size and morphologies.

Also, Fig. 10 shows the variation of the cooling rate with the powder particle sizes obtained in this study for both stages I and II solidification.

As shown in Fig. 10, It is clear that the cooling rate reduces as the particle size increases. Moreover, the cooling rate for stage I varies between $4.9 \times 10^3 - 2.8 \times 10^6$ K/s with solidification time ranging from 220 – 0.388 Ns whereas the cooling rate ranges between $6.2 \times 10^4 - 3.4 \times 10^7$ K/s for solidification time varying between 17.3 – 0.031Ms. The SEM micrographs showing a spectrum of particle shapes for aluminium powder are presented in Fig. 11 while the particle size and distribution characteristics of the powder obtained from SEM analysis is shown in Fig. 12.



(a) Powder produced at 45° incidence angle



(b) Powder produced at 40° incidence angle.

Fig. 11: SEM micrographs showing a spectrum of particle shapes for aluminium powder produced

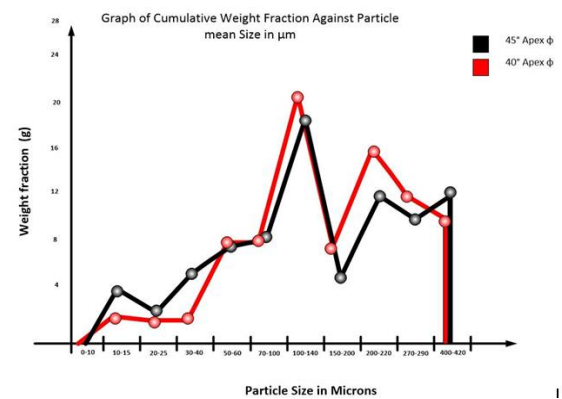


Fig. 12: Graph of weight fraction against particle size distribution of the aluminium powders obtained in this study.

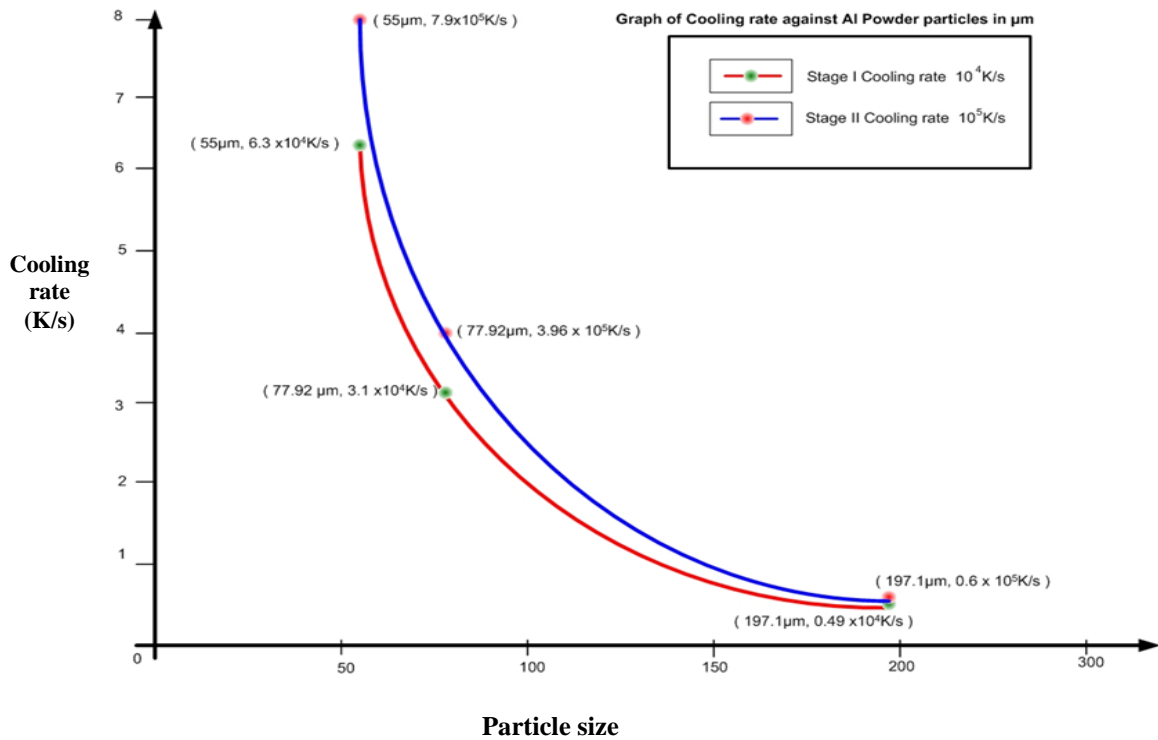


Fig. 10: Variation of the cooling rate with the powder particle sizes for stages I and II solidification.

Table 2. Sauter (Dvs), Volume (Dvm) Mean Diameter and Yield of (Bulk) Aluminium Powder Using sieve Analysis

Incidence or Apex Angle	DVS(μm)	DVM(μm)	D50(μm)	weight (kg)	Yield	yield%
45°	80.31	172.49	115	0.2611	0.27850667	27.85066
40°	62	165	95	0.6764	0.72149333	72.14933
Total				0.9375		

As shown in Fig 11 (a and b), it can be observed that the aluminium particles produced an irregular morphology from the air atomiser for incidence 40° and 45° respectively. It is clear that powders having particle size distribution of 3 – 197 μm for incidence angle 40° and 4 – 260 μm for incidence angle 45° were obtained from the equipment. Also, the results obtained from the SEM micrograph taken for powders produced using different incidence angles is as shown above. There were differences in morphologies and atomization at incidence of 45° reveals elongated morphologies compared to powders produced by an incidence of 40° with more spherical morphologies. Also, Table 2 shows that powders produced with

the incidence angle of 40° have the higher yield of 72% compared to 45° with 27.85% under same atomizing parameter conditions.

4.0 CONCLUSION

The following conclusions were drawn from this study:

- Geometrical intersection of high velocity atomizing medium with melt stream causes instability and drastic cooling at the nozzle tip for close-coupled nozzles.

- ii. Also, caking at the nozzle tip of close-coupled nozzles is more pronounced from 45° incidence angle.
- iii. Atomization was carried out in the developed laboratory scale atomizer under the same atomizing conditions and the powders produced by two close-coupled nozzles at 40° as well as 45° respectively differs in size and morphology.
- iv. Similarly, powders produced with close-coupled nozzles at 45° incidence tend to be larger in particle mean size while powders produced with closed-coupled nozzle at 40° are narrower in particle mean size
- v. Finally, close coupled nozzles at incidence angle of 40° produce more powder quantity compared to the close-coupled nozzles at 45°.

REFERENCES

- [1] Morakotjinda, M., Fakpan, K., Yotkaew T., Tosangthum, N., Krataithong R., Daraphan A., Siriphol, P., Wila, P., Vetayanugul, B., and Tongsri, R. (2010). Gas atomization of low melting-point metal powders. *Chiang Mai J. Sci.* 37(1), 2010: 55-63.
- [2] Fugian, Z., Ming, V., Jianliang, L., Xianyoung, L., Weiming, G., An, S., Zhongmin D. (2001). "Study of rapidly Solidified atomization Techniques and production of metal alloy powders institute of precious metal", *Materials Science and Engineering A304-306*, 579-582.
- [3] Lagutkin, S., Achelis, L., Sheikhaliev, S., Uhlenwinkel, V., Srivastava, V., (2004). "Atomization process for metal powder. *University Bremen*", *Germany. A 383(2004)* 1-6.
- [4] Eslamian, M., Rake, J., Ashgriz, N. Preparation of aluminium/silicon carbide metal matrix composites using centrifugal atomization " *Powder Metallurgy* " 184 (2008) pp 11-20
- [5] Yang, M., Dai, Y., Song, C., Zhai, Q., (2009) " *Journals of Materials processing Technology* ". Pp. 1-5
- [6] Vojtech, O., Prusa, F., Michalcova, A., (2010) " *Journal of alloys and compound* " 506 pp 581-588.
- [7] Anderson, I. E., Terpstra, R.L., and Rau, S. Progress toward understanding of gas atomization processing physics, in: K. Bauckhage, V. Uhlenwinkel (Eds.), *Spray Forming, Kolloquium Band 5, Books on Demand GmbH* (ISBN 3-88722-508-2), Norderstedt, 2001, pp. 1-16.
- [8] Lubanska, H., (1970). " *Correlation of spray Ring Data for gas atomization of liquid metals* ", *J. met.*, Vol. 22 no. 2 pp. 45-49
- [9] Planche, M.P., Allimant, A., Bailly, Y., Dembinski, L., Coddet, E., (2009). "Progress in gas atomization of liquid metals by means of a De Laval nozzle". *Powder Technology 190(2009)* pp 79-83
- [10] Stobik, M. (2002). Nanoval atomizing: capabilities, applications and related processes, In: *Kolloquium Sprühkompaktieren/ Spray forming, Bauckhage and Uhlenwinkel, Bremen, Germany*, 6, pp. 65-80.
- [11] Mates, S.P. & Settles, G.S. (2005). A study of liquid atomization using close-coupled nozzles, Part 1: Gas dynamic behaviour, *Atomization and Sprays* 15 (1), 19-40
- [12] Agada, S.O. (2013) Design and Construction of Laboratory scale atomizer for producing Aluminium powder. Masters project, Federal University of Technology Minna Niger State Nigeria. *Unpublished*.
- [13] Dombrowski, N. & Johns, W.R. (1963). The Aerodynamic Instability and Disintegration of viscous. *Liquid Sheets Chem. Eng. Scie.* 18. 203-